TOPOLOGICAL OPTIMIZATION OF THE ROCKER ARM

ELISKA POSMYKOVA, MAREK GAZDA, JAKUB MESICEK

Department of Machining Assembly and Engineering Metrology, Faculty of Mechanical Engineering, VSB -Technical University of Ostrava, Ostrava, Czech Republic

DOI: 10.17973/MMSJ.2023_06_2023036

eliska.posmykova.st@vsb.cz

The focus of this paper is to compare the results of topological optimization (TO) of the rocker arm for following 3D printing out of AISI 316L stainless steel by the Selective Laser Melting (SLM) method. We used the Altair Inspire software to optimize the shape of the rocker arm. Two variants of optimization were created, first, a variant of optimization without the Shape Control function was carried out, which resulted in a complex mechanical component with an organic shape. This bionic design means more support for the SLM method of Additive Manufacturing (AM) and worse surface quality after their removal. Therefore, a second variant of optimization was produced with the application of the Shape Control function, which positively affects manufacturability and postprocessing. The use of shape control reduced the amount of supports to a minimum, helping to improve the surface finish.

KEYWORDS

Additive manufacturing, SLM, AISI 316L, topological optimization

1 INTRODUCTION

The aim of the work is to perform topological optimization of the shape of the specified component – rocker arm – in the Altair Inspire software. First, the production conditions for the rocker arm were determined (what technology will be produced, how many pieces, budget for production, and rocker arm parameters), because all these parameters will affect the choice of material and affect the optimization itself [Antar 2022].

Topological optimization (TO), as a tool for calculating the distribution of the material in the volume of a component, helps to reduce weight while maintaining mechanical properties [Kudrna 2022]. The TO methods are increasingly used in the field of 3D printing. First, the production conditions for the rocker arm were determined (the part will be manufactured using the Selective Laser Sintering (SLM) technology, the number of components to be fabricated, the budget for production, and the dimensions of the component), because all these conditions will affect the choice of material and the optimization itself [Kozior 2022].

The Altair Inspire software uses Solid Isotropic Material with the Penalization (SIMP) method. The SIMP method is directly based on the homogenization method, which is an indirect optimization method and is mostly used as a form of shape optimization. The main purpose of this method is to find the optimal distribution and shape of the material [Hlinka 2020].

2 TOPOLOGICAL OPTIMIZATION OF THE COMPONENT

There have been established goals for topological optimization that the optimized component must accomplish. For a modified, optimized part, we require the same (or less) maximum displacement as the original part. The minimum factor of safety of the optimized part must not be less than that of the original part. Also at least 20% weight savings are required compared to the original part [Kudrna 2022].

The main purpose of this method is to find the optimal distribution and shape of the material [Hlinka 2020].

The production conditions were determined, the functional surfaces of the rocker arm would be preserved, and the prototype would be manufactured using SLM metal 3D printing technology with AISI 316L stainless steel. The rocker arm is loaded with a force F = 750 N as shown in Fig. 1. We performed a strength analysis of the original part. The results and discussions section further defines the fulfillment of these additional conditions. We performed the first optimization and subsequent check using strength analysis [Jenkins 2015].

2.1 The choice of material

Materials were compared according to the values in Tab 1. and select the most suitable material. For example, the height of the layer affects the print speed (energy consumption and thus the price of the product) and the quality of the surface [Mesicek 2021].

Table 1. Mechanical properties of materials used for 3D printing with SLM technology.

Material	AISI 316L	ALSi10Mg	Ti6Al4V	In718	Maraging Steel
Average density [$kg \cdot m^{-3}$]	8000	2600	4420	8190	8100
Layer thickness [µm]	50	25	30/60	30/60	40
Yield strength $R_{p0.2}$ [MPa]					
Horizontal	662	400	1100	1400	1800
Vertical	580	340	1060	1340	1794
Tensile strength R_m [MPa]					
Horizontal	520	265	980	725	1030
Vertical	494	240	890	650	950
Young modulus [GPa]					
	190	68	114	200	210

Firstly, the aluminum alloy printing material AlSi10Mg was selected due to affordability. However, we must have verified whether the rocker arm made of this material will meet the specified conditions [Adamczak 2017].

Then the material AISI 316L stainless steel was chosen due to a higher Young modulus value of 190 GPa, and at the same time it is comparable in price to the original AlSi10Mg alloy [Kudrna 2022].

The optimal material for our component was chosen. Subsequently, the selection of the material was checked using a strength analysis in the Altair Inspire software [Kozior 2022].

2.2 Strength analysis of the original part

We have added a force effect that acts on the small hole of the rocker arm – the Bearing Force function under the Loads tab was used and the force value was set as specified to F = 750 N shown by the red arrow in Fig. 1. This force F acts downwards and is distributed over the lower part of the smaller cylindrical hole [Mesicek 2021].

Figure 1: Location of the load force applied to the rocker arm.

We performed a strength analysis using the Finite Element Method (FEM) of the original part. We entered in the analysis parameters that we want to Minimize Mass [Zhang 2017].

During the analysis, we monitor the following parameters:

Factor of safety – The aim is that the minimum value of the factor of safety is 3. According to the analysis of the original part, the actual factor of safety is equal to 3.1. The condition is therefore met [Wang 2022].

Displacement – the maximum displacement that must be maintained even with an optimized part is $2 \cdot 10^{-2}$ mm. Therefore, the maximum displacement of the optimized part must be less than or equal to $2 \cdot 10^{-2}$ mm.

von Misses Stress – The maximum von Misses is 66MPa at the area indicated in Fig. 2.

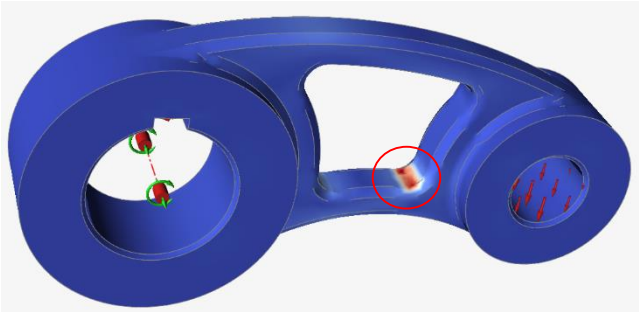

Figure 2: von Misses stress.

2.3 Definition of Design Space

Optimization software requires simplification of the optimized component for a smooth simulation process. We made changes to the model of the rocker arm component so that we could perform topological optimization. These changes include increasing the width of the rib between the two cylindrical parts, removing chamfers, and replacing them with sharp edges [Cervinek 2021].

Fig. 3 shows the changes made to the rocker arm model that were mentioned before.

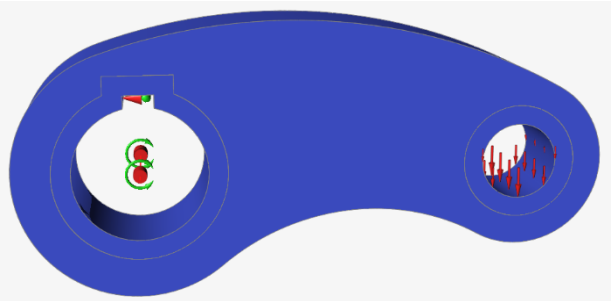

Figure 3: Definition of Design Space.

2.4 Topological optimization parameters

After the analysis, we proceeded to optimization, where we entered the input parameters:

- minimum factor of safety: 3.1
- minimize the mass of the part

The goal of the optimization is to minimize weight, consequently, the Minimize Mass option in the Altair Inspire software was chosen. The first attempt at optimization was unsatisfactory in terms of the strength of the part, therefore it was done again with the aim of maximizing stiffness. The result can be seen in Fig. 4.

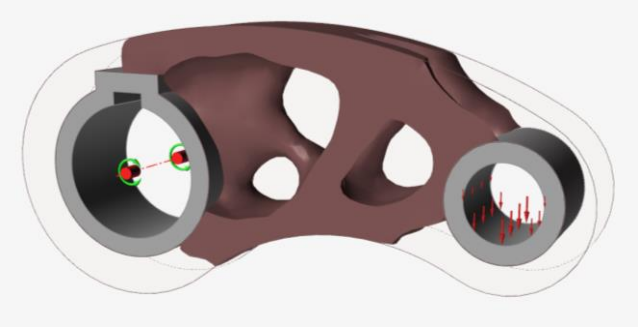

Figure 4: The first suitable variant of optimization.

The PolyNURBS function was then used on the first optimized design to create a smooth geometry. The result of this process is shown in Fig. 5.

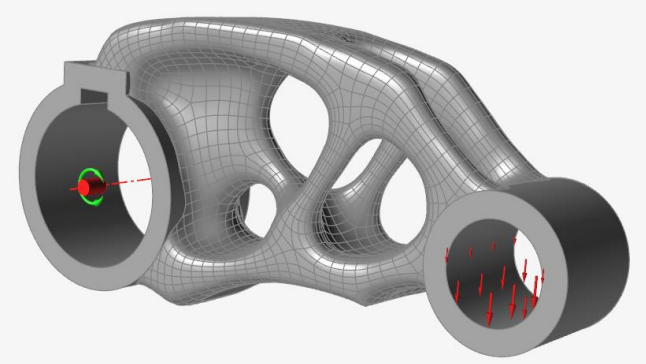

Figure 5: The first variant of optimization with the application of conversion to PolyNURBS surfaces.

2.5 Conditions of manufacturability

The resulting model is in the form of an optimized bionic structure with an attractive design. For our chosen production technology (SLM), this organic, nature-inspired shape would need a lot of supports to enable the 3D process [Yago 2022]. This would result in impaired surface quality and more demanding and lengthier postprocessing [Allaire 2004].

Therefore, a second variant of optimization was produced with the application of the shape control function, which positively affects manufacturability and postprocessing. The use of shape control reduced the amount of supports to a minimum, helping to improve the surface finish [Previati 2019].
In the production of SLM technologies, the rocker arm would be placed in the printing chamber so that the axes of the holes are perpendicular to the print bed, as shown in Fig. 6. This condition is taken into account by the Shape Control – Extrude function. The part must still be connected to the print bed by supports, but there will be significantly fewer of them than in the case of the first variant of optimization [Yago 2022].

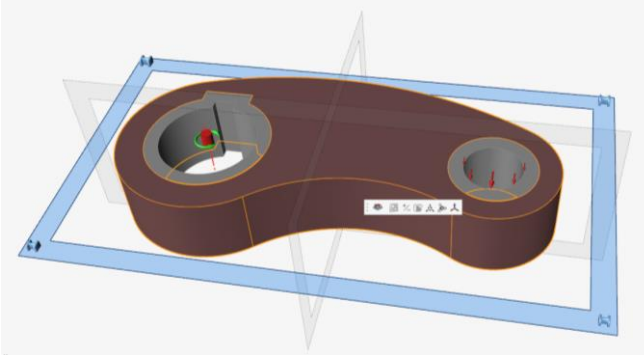

Figure 6: Application of manufacturability conditions to the rocker arm component.

This variant was also tested by strength analysis as shown in Fig. 7. The maximum displacement is $1.145 \cdot 10^{-5}$ mm, it does not exceed the permissible limit (which is 0.02 mm), and the optimized rocker arm with the set extrusion conditions is suitable.

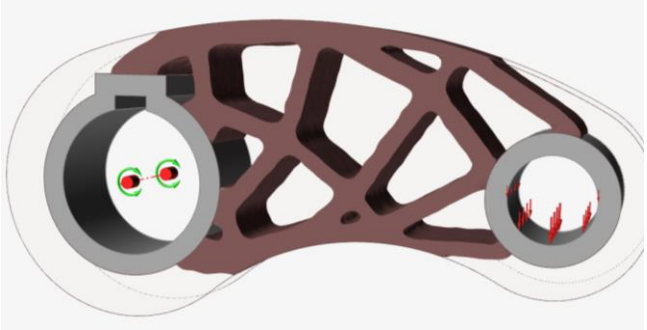

Figure 7: The new shape of the part with the application of the Shape Control function.

The PolyNURBS function was then used on the first optimized design to create a smooth geometry. The comparison of PolyNURBS model's visual results can be seen in Fig. 8.

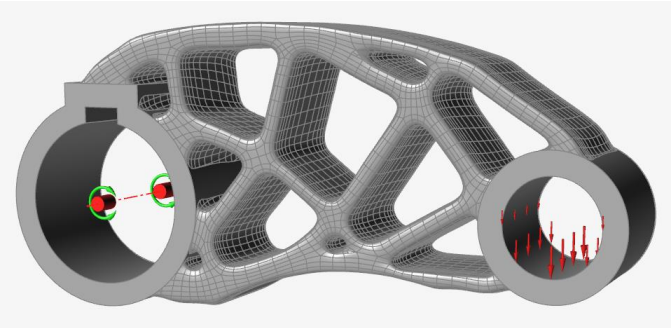

Figure 8: The second variant of optimization.

The comparison table (Tab. 2) and graph (Fig. 9) show that the condition of reducing the mass by at least 20% of the weight is met compared to the original model. With the first variant of optimization, the weight saving is 39.63%. For the second variant, it is 34.10%. In Fig. 9. We can see the comparison of mass and the factor of safety for the original part and the first and second variant of optimization [Wang 2022].

Table 2. Comparison of the achieved results of the original part and two optimization variants.

	Original part	The first variant of optimization	The second variant of optimization
Mass [kg]	0.8933	0.5393	0.5891
Factor of safety [-]	3.1	8.3	15.4
Maximal displacement [mm]	$2{,}458 \cdot 10^{-2}$	$1{,}130 \cdot 10^{-5}$	$1{,}145 \cdot 10^{-5}$

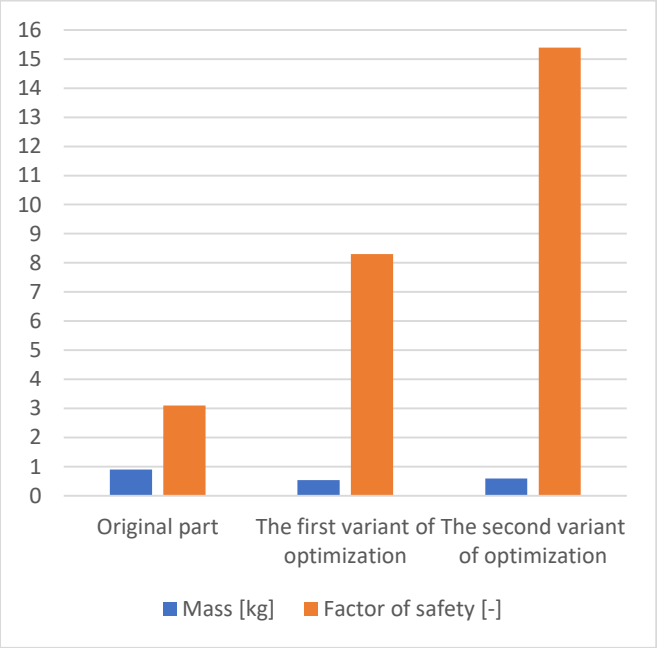

Figure 9: Comparison of the achieved results of the original part and two optimization variants.

2.6 Comparison of the two variants of topological optimization

The rocker arm models were sliced (the original part, the first and the second variant of optimization). Supports have been generated on the models to produce SLM technologies on the Renishaw Ren AM 500M 3D printer from 316L stainless steel. The orientation in the print chamber of both variants is similar – the hole axes are perpendicular to the print bed. This ensures the smallest possible height of the print structure in the Z-axis, making the build as short as possible and consuming as little energy as possible.

A comparison of the three variants of the rocker arm was made in terms of the amount of supports during the above-mentioned print orientation. The following parameters were monitored: the area of the model to be supported – Support Area, Support Volume, and the printing time for the whole part – Printing Time.

The results of the comparison are mentioned in Tab. 3. It is obvious that the original model has the largest surface area that needs to be secured by supports, the largest volume of supports, and the longest printing time, which is undesirable.

Table 3. Comparison of the achieved results of the original part and two optimization variants.

	Original part	The first variant of optimization	The second variant of optimization
Support Area [mm^2]	12 435	11 087	9 630
Support Volume [mm^3]	218 000	194 000	168 000
Printing Time [s]	12 690	11 622	10 466

The first variant of optimization shown in Fig. 10 has both a smaller Support Area and Support Volume compared to the original part, as presented in Table 3. However, due to the complex shape of this part, the subsequent removal of supports is difficult and leads to a degradation in surface quality at the contact surfaces between the supports and the model [Sotola 2021].

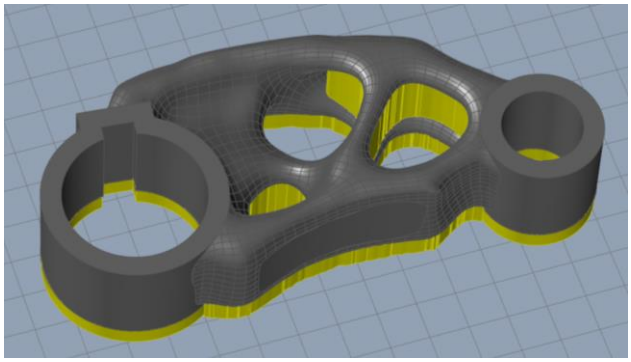

Figure 10: The first variant of optimization with Supports.

The first variant of optimization shown in Fig. 10 has both a smaller Support Area and Support Volume compared to the original part, as presented in Table 3. However, due to the complex shape of this part, the subsequent removal of supports is difficult and leads to a degradation in surface quality at the contact surfaces between the supports and the model [Antar 2022].

The second variant of optimization, in which the Shape Control function was applied, can be seen in Fig. 11. The Shape Control ensures the easiest manufacturability of the part. The second optimization variant has a significantly reduced Support Volume compared to the original rocker arm. The printing time in this case is greatly reduced as shown in Tab. 3.

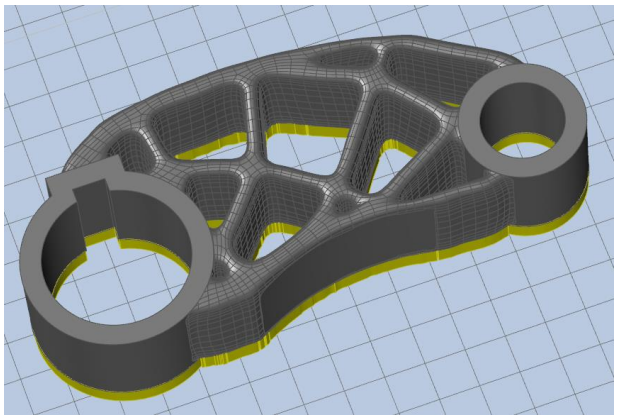

Figure 11: The second variant of optimization with Supports.

3 CONCLUSIONS

If we evaluate the results of optimizations from the strength point of view, both component variants are satisfactory, as each optimization variant has been checked using the FEM analysis of Altair Inspire [Shevchenko 2022].

Further in the process, we applied the condition of manufacturability (shape control) from which the second and final optimization variant emerged, which was transferred to the NURBS model. The TO results were summarized utilizing the PolyNURBS function in Altair Inspire software, which can be exported into other CAD formats [Previati 2022].

However, it is preferable to choose the second variant over the first variant because of the reduction of supporting material. We can clearly see from Fig. 9. that the second variant of optimization has the highest factor of safety with a value of 15.4. The mass of the second variant of optimization is reduced by more than 20 % to 0.5891 kg. The maximal displacement of the second variant has been reduced to $1{,}145 \cdot 10^{-5}$ mm (as seen in Tab. 2.) which is significantly smaller than the displacement of the original part. Due to these results and better manufacturability, it is more suitable to choose the second variant of optimization. It is appropriate and highly important to consider the component's manufacturability and subsequent postprocessing when using topological optimization tools [Zhang 2017].

ACKNOWLEDGMENTS

This paper was completed in association with the project Innovative and additive manufacturing technology - new technological solutions for 3D printing of metals and composite materials, reg. no. CZ.02.1.01/0.0/0.0/17_049/0008407 financed by Structural Funds of the European Union. The article has been done in connection with the project Students Grant Competition SP2023/088 „Specific Research of Modern Manufacturing Technologies for Sustainable Economy“ financed by the Ministry of Education, Youth and Sports and Faculty of Mechanical Engineering VŠB-TUO.

REFERENCES

[Adamczak 2017] Adamczak, S.; Zmarzły, P.; Kozior, T.; Gogolewski, D. Assessment of roundness and waviness deviations of elements produced 649 by selective laser sintering technology. In Proceedings of the 23rd International Conference Engineering Mechanics, Svratka, 650 Czech Republic, 15 – 18 May 2017.

[Allaire 2004] Allaire, G., Jouve, F. & Toader, A.-M. (2004). Structural optimization using sensitivity analysis and a level-set method. *Journal of Computational Physics*, *194*(1), 363–393. https://doi.org/10.1016/j.jcp.2003.09.032

[Antar 2022] Antar, I., Othmani, M., Zarbane, K., El Oumami, M. & Beidouri, Z. (2022). Topology optimization of a 3D part virtually printed by FDM. *Journal of Achievements in Materials and Manufacturing Engineering*, *112*(1), 25–32. https://doi.org/10.5604/01.3001.0016.0289

[Cervinek 2021] Cervinek, O., Koutny, D., Vaverka O., Pantelejev, L. and Palousek, D. (2021). Computational Approaches of Quasi-Static Compression Loading of SS316L Lattice Structures Made by Selective Laser Melting. Materials, 14(9) 2462. https://doi.org/10.3390/ma14092462

[Hlinka 2020] Hlinka, J., Kraus, M., Hajnys, J., Pagac, M., Petru, J., Brytan, Z. & Tanski, T. (2020). Complex Corrosion Properties of AISI 316L Steel Prepared by 3D Printing Technology for Possible Implant Applications. *Materials*, *13*(7), 1527. https://doi.org/10.3390/ma13071527

[Jenkins 2015] Jenkins, N. & Maute, K. (2015). Level set topology optimization of stationary fluid-structure interaction problems. *Structural and Multidisciplinary Optimization*, *52*(1), 179–195. https://doi.org/10.1007/s00158-015-1229-9

[Kozior 2022] Kozior, T., Bochnia, J., Gogolewski, D., Zmarzły, P., Rudnik, M., Szot, W., Szczygieł, P. & Musiałek, M. (2022). Analysis of Metrological Quality and Mechanical Properties of Models Manufactured with Photo-Curing PolyJet Matrix Technology for Medical Applications. *Polymers*, *14*(3), 408. https://doi.org/10.3390/polym14030408

[Kudrna 2022] Kudrna, L., Ma, Q.-P., Hajnys, J., Mesicek, J., Halama, R., Fojtik, F. & Hornacek, L. (2022). Restoration and Possible Upgrade of a Historical Motorcycle Part Using Powder Bed Fusion. *Materials*, *15*(4), 1460. https://doi.org/10.3390/ma15041460

[Mesicek 2021] Mesicek, J., Jancar, L., Ma, Q.-P., Hajnys, J., Tanski, T., Krpec, P. & Pagac, M. (2021). Comprehensive View of Topological Optimization Scooter Frame Design and Manufacturing. *Symmetry*, *13*(7), 1201. https://doi.org/10.3390/sym13071201

[Previati 2019] Previati, G., Ballo, F. & Gobbi, M. (2019). Concurrent topological optimization of two bodies sharing design space: problem formulation and numerical solution. *Structural and Multidisciplinary Optimization*, *59*(3), 745–757. https://doi.org/10.1007/s00158-018-2097-x

[Previati 2022] Previati, G., Ballo, F. & Gobbi, M. (2022). A shape function based interpolation approach for nodal design variable based structural optimization. *International Journal for Numerical Methods in Engineering*, *123*(11), 2660–2675. https://doi.org/10.1002/nme.6954

[Shevchenko 2022] Shevchenko, S. Yu. & Mikhailenko, D. A. (2022). Topological Optimization of Circular SAW Resonators: Overcoming the Discreteness Effects. *Sensors*, *22*(3), 1172. https://doi.org/10.3390/s22031172

[Sotola 2021] Sotola, M., Marsalek, P., Rybansky, D., Fusek, M. & Gabriel, D. (2021). Sensitivity Analysis of Key Formulations of Topology Optimization on an Example of Cantilever Bending Beam. *Symmetry*, *13*(4), 712. https://doi.org/10.3390/sym13040712

[Wang 2022] Wang, X., Qin, R. & Chen, B. (2022). Mechanical properties and energy absorption capability of a topology-optimized lattice structure manufactured via selective laser melting under axial and offset loading. *Proceedings of the Institution of Mechanical Engineers, Part C: Journal of Mechanical Engineering Science*, *236*(19), 10221–10236. https://doi.org/10.1177/09544062221100614

[Yago 2022] Yago, D., Cante, J., Lloberas-Valls, O. & Oliver, J. (2022). Topology Optimization Methods for 3D Structural Problems: A Comparative Study. *Archives of Computational Methods in Engineering*, *29*(3), 1525–1567. https://doi.org/10.1007/s11831-021-09626-2

[Zhang 2017] Zhang, S., Gain, A. L. & Norato, J. A. (2017). Stress-based topology optimization with discrete geometric components. *Computer Methods in Applied Mechanics and Engineering*, *325*, 1–21. https://doi.org/10.1016/j.cma.2017.06.02

CONTACTS:

Eliska Posmykova
VSB -Technical University of Ostrava
Faculty of Mechanical Engineering
Department of Machining Assembly and Engineering Metrology
17. listopadu 2172/15, Ostrava, 708 00, Czech Republic
eliska.posmykova.st@vsb.cz